Available online at www.sciencedirect.com
SCIENCE DIRECT®
Journal of Power Sources 137 (2004) 216–221
JOURNAL OF POWER SOURCES
www.elsevier.com/locate/jpowsour

Short communication

Enhancement of hydrogen oxidation activity at a nickel coated carbon beads electrode by cobalt and iron

A.K. Chatterjee [a,*], R. Banerjee [a], M. Sharon [b]

[a] *Energy Systems Engineering, Indian Institute of Technology Bombay, Powai, Mumbai 400076, India*
[b] *Nano Technology Research Lab, Birla Collage, Kalyan, Maharashtra, India*

Received 12 March 2004; accepted 28 May 2004
Available online 14 August 2004

Abstract

The electrochemical characteristics of a porous ceramic that is coated with carbon beads, impregnated with Ni, Fe and Co catalyst and operated as a hydrogen electrode for an alkaline fuel cell (AFC) are studied. To improve the catalytic activity and electrode performance, Ni is bimetallized with Co as well as Fe. Chemical vapour deposition (CVD) of turpentine oil, a renewable natural precursor, is used to grow the carbon beads. Various compositions of Ni–Co and Ni–Fe (10:90, 50:50, 90:10) are electroplated over the carbon-coated ceramic substrate. The detailed surface profile and elemental composition of the electrodes are studied by SEM, TEM, XRD and XRF analysis. Vander–Pauw resistivity measurements of the electrodes showed an increase in the conductivity of Ni electrode by addition of Co and Fe. The electrochemical performance is investigated by measuring hydrogen dissociation voltage, half-cell and full-cell current–potential characteristics and chrono-potentiometry in 30% KOH solution. The activity of the NI electrode is improved by addition of small amounts of Co and Fe. The best performance is obtained using an electrode coated with 90:10 ratios of Ni–Co and Ni–Fe bimetallic composition.

Keywords: Carbon beads; Hydrogen electrode; Nickel-coated ceramic; Iron and cobalt catalyst; Alkaline fuel cell; Electrocatalyst

1. Introduction

Environmental pollution resulting from the combustion of fossil fuels has led to a demand for the development of new, clean, energy systems. Fuel cells, which convert the chemical energy of a fuel continuously into electrical energy, are promising choices due to their low pollution and high efficiency [1,2]. Among the different fuel cell technologies, the alkaline fuel cell (AFC) was the first to be put into practical service [3]. Starting with applications in space the alkaline cell provided high-energy conversion efficiency with no moving parts and high reliability [3,4]. In addition, cost AFC electrodes may be prepared from non-noble metal catalysts [5] which reduces cost. PTFE bonded Raney Nickel has been widely used as an efficient electrocatalyst in AFCs [6]. Although this material has excellent hydrogen adsorption ability and relatively large surface area, it suffers the disadvantage of a high electrolyte diffusion resistance due to a low pore volume and small pore size [7]. In order to increase strength, excess PTFE is added. This makes the electrode completely hydrophobic with high resistance and prevents the flooding of the agglomerates [8,9]. Highly conducting carbon materials with evenly dispersed electrocatalysts can eliminate these difficulties, provided a method is developed to increase the porosity of the carbon. Recently, Ni-coated carbon nanobeads over a porous ceramic have been shown [10] to give good performance in AFCs. Bimetallic compositions may, however have better performance than mono metal electrocatalysts due to their modified surface characteristics [11,12]. The catalytic enhancement by bimetallic surfaces may be due to bifunctional, ligand (electronic) or morpbological effects.

In this study, the electrocatalytic performances of bimetallic Ni–Co and Ni–Fe are evaluated. Ni–Co and Ni–Fe with different proportions are electrodeposited over carbon beads that, in turn, are coated over a porous ceramic substrate.

2. Experimental

Carbon beads were grown over a ceramic substrate by a chemical vapour deposition (CVD) method. The CVD unit

* Corresponding author. Tel.: +91-22-25767890; fax: +91-22-25764890.
E-mail address: akchatterjee@iitb.ac.in (A.K. Chatterjee).

0378-7753/$ – see front matter © 2004 Elsevier B.V. All rights reserved.
doi:10.1016/j.jpowsour.2004.05.061

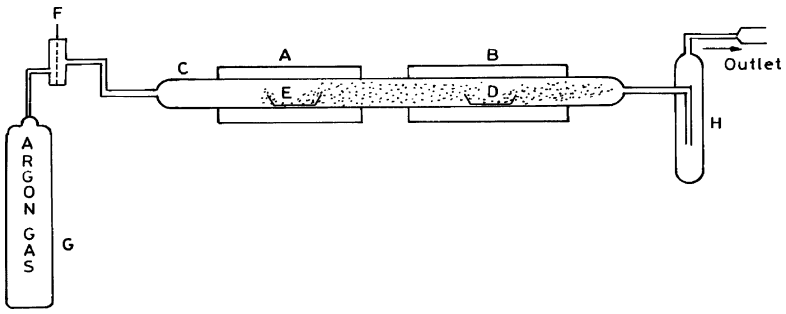

Fig. 1. Schematic diagram of chemical vapour deposition equipment: (A) vaporising furnace; (B) pyrolysing furnace; (C) quartz tube; (D) quartz boat with ceramic substrate; (E) quartz boat with precursor; (F) flow regulator; (G) gas cylinder; (H) gas bubbler.

consisted of two furnaces joined side by side with a quartz tube traversing both of them (Fig. 1). The furnace (A) was used to vaporize turpentine oil (natural precursor) and the furnace (B) to pyrolyse the turpentine oil vapour. The vapour was carried over from A by a stream of argon gas. A quartz boat (E) that contained 2 ml of turpentine oil was placed in furnace A, and maintained at 200 °C. The temperature of furnace (B), which housed a quartz boat (D) with the ceramic substrate, was maintained at 900 °C. After deposition, the furnaces were cooled and the ceramic substrate coated with carbon from the boat D was collected. Ni, Co, Fe and their different bimetallic compositions (Ni–Co, Ni–Fe) were electroplated from their respective metal nitrate solution on carbon beads deposited over porous ceramic substrate. Three ranges (10:90, 50:50, 90:10) of bimetallic composition were chosen. The binary solution for electrolysis was prepared from the individual molar solution in the required ratio. Electrodes thus prepared were reduced from their oxides into metal in a hydrogen atmosphere at around 450 °C for 3 h into the electrochemical cell.

The surface morphology of the carbon beads coated over the ceramic substrate was studied using SEM and TEM. The SEM morphological examination of electrodes was carried out with a JEOL JSM-840 instruments, while TEM micrographs were obtained with a Philips CM-200 instrument. The nature of the carbon beads and the electrocatalysts were examined by XRD analysis (Philips 1790 X-ray diffractometer, Cu Kα radiation). The XRD pattern of the ceramic substrate was subtracted from the XRD pattern of the ceramic substrate deposited with carbon beads and coated with electrocatalyst. The presence of metal catalyst on the electrode was also confirmed by XRF analysis. To measure the conductivity of electrodes, the variation of resistance with respect to temperature was recorded in an argon atmosphere by the Vander–Pauw method. The electrochemical performance of the electrodes was investigated by using them as working electrodes in an AFC. The hydrogen dissociation voltage and half-cell and full-cell current–voltage characteristics and chrono-potentiometry were measured with a Pine potentiostat AFRDE4.

The half-cell had a three-electrode configuration with a standard calomel electrode (SCE) as reference electrode, platinum as the counter electrode, and the carbon beads coated metal electrode as the working electrode, i.e., hydrogen electrode, H_2|30% KOH|SCE|Pt. Using the same configuration, half-cell characteristics were studied and chrono-potentiometry was performed. For full-cell characteristics, a silver deposited carbon beads electrode was used as the cathode and a hydrogen electrode as the working electrode with configuration: Hydrogen electrode, H_2|30% KOH| oxygen electrode, O_2.

3. Results and discussion

Scanning and transmission electron micrographs of the ceramic coated with carbon without using any electrocatalyst are shown in Figs. 2 and 3, respectively. These micrographs reveal the presence of highly dense and interconnected carbon beads spread over the surface of the ceramic. These beads have a diameter in the range of 500–650 nm, and are interconnected with graphitic layers that engulf a few beads. The significant peaks of XRD patterns of the electrodes are shown in Figs. 4 and 5. The peaks at 26.60 (0 0 2), 68.02 (1 0 1) and 41.105 (0 0 4) clearly reveal that the carbon beads are graphitic in nature. Peaks in Fig. 4(c) for Ni(1 1 1), (2 0 0) and (2 2 0) are seen clearly in Fig 4(a) whereas Co prominent peaks (1 1 1) and (2 2 0) are seen in Fig. 4(b) Bimetallic overlapping peaks of Ni and Co are prominent in Fig. 4(c) which indicates structural reconstruction of the metal lattices. Peaks of Co(1 0 0) at 41.43, Ni(1 1 1) at 44.75, Ni(2 0 0) at 51.96 are shown in Fig. 4(e) along with Ni(2 2 0) and Co overlapping peaks at 76.60 with high relative intensities. It is interesting to note that the bimetallic electrocatalyst suppressed the C(0 0 4) plane, as shown in Figs. 4(a) and (b), 5(a) and (b). The XRD patterns of Ni, Fe and their bimetallic alloys compositions are compared in Fig. 5. The XRD patterns of only Ni and Fe coated bead electrodes are presented in Fig. 5(a). In Fig. 5(e), at 31.01 (undefined), 43.58 (1 1 1), 65.00 (2 0 0) intense peaks are noted for a Ni–Fe composition. In addition to the carbon peaks, peaks for Ni (51.385) and Fe (44.115) are also noted. In Fig. 5(d) peaks at 31.055 (Ni–Fe) and at 65.00 (Ni–Fe) (2 0 0) correspond to the alloy composition for a high percentage of Fe (90%), a prominent peak is formed at 43.58. These XRD patterns clearly show the bimetallic alloy formation of the

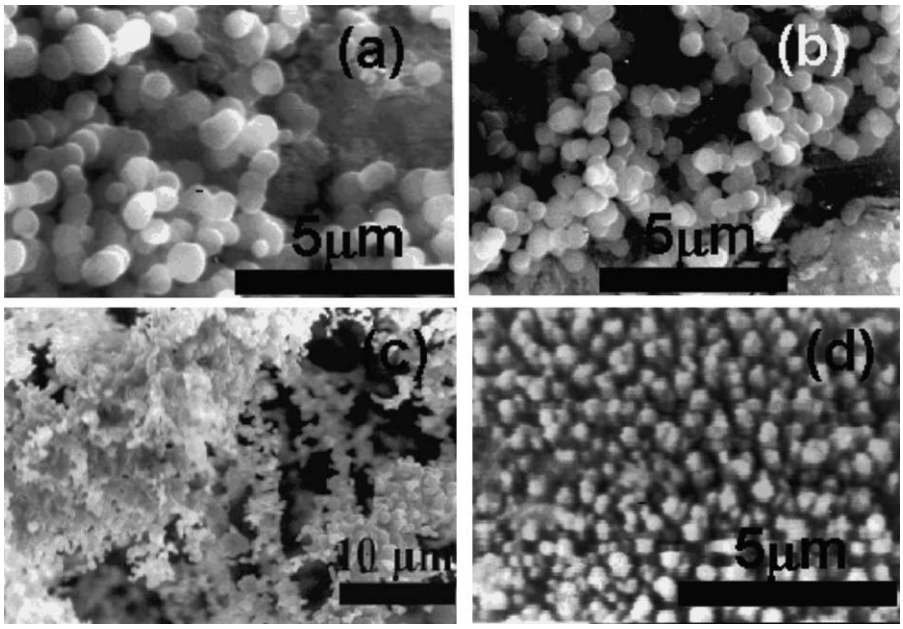

Fig. 2. Scanning electron micrographs of carbon beads: (a) and (b) without catalyst; (c) coated with Ni catalyst; (d) coated with Co catalyst.

electrocatalysts and their composition. Such Ni–Fe alloy formation protects the electrocatalysts from corrosion. These, XRD data also confirm the presence of respective metals and their constituents. Vander–Pauw resistivity data are given in Table 1. The variation in resistance of the electrodes with respect to a temperature gradient in an argon atmosphere is presented in Fig. 6. The data indicate that the electrodes are highly conducting. Moreover, there is little change in resistance with temperature, which demonstrates the high thermal stability of the electrode. It is also observed that addition of Co and Fe to the Ni increases the conductivity of electrodes.

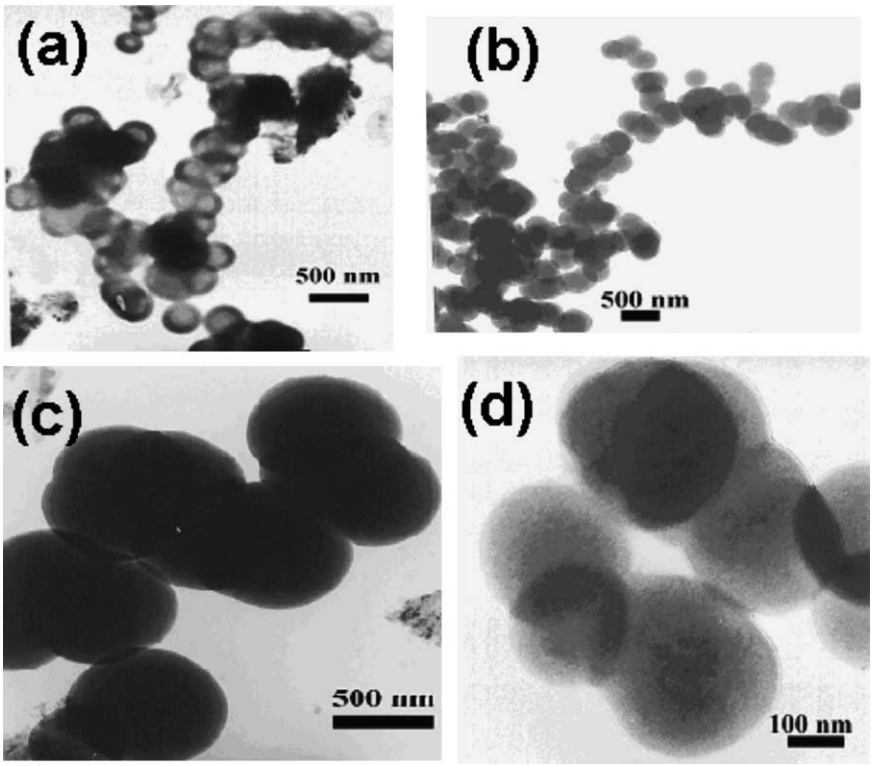

Fig. 3. Transmission electron micrographs of carbon beads at different magnification showing porous structures.

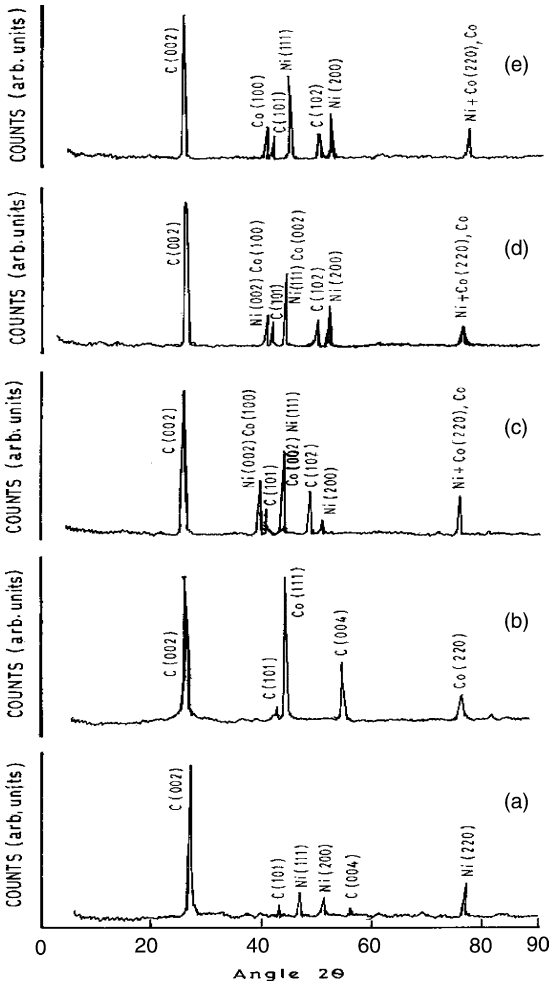

Fig. 4. XRD pattern of Ni + Co electrodes: (a) Ni; (b) Co; (c) Ni–Co (50:50); (d) Ni–Co (50:50); (e) Ni–Co (90:10).

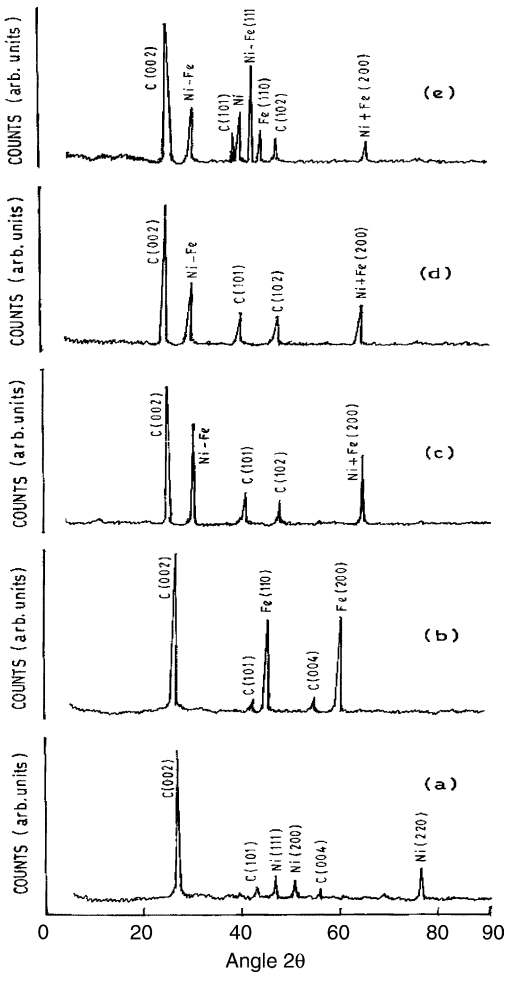

Fig. 5. XRD pattern of Ni + Fe electrodes: (a) Ni; (b) Co; (c) Ni–Fe (10:90); (d) Ni–Fe (50:50); (e) Ni–Fe (90:10).

The hydrogen dissociation voltages of the electrodes measured with respect to a SCE are listed in Table 1. A high H_2 dissociation voltage of −982 mV was recorded for electrode with Co (10%) and Ni (90%), whereas for only Ni its value was −956 mV. This suggests that Co helps to reduce the reduction potential for hydrogen either by either by improving electrocatalystic behaviour of Ni or by decreasing the resistance of the Ni-coated electrode. The current–voltage characteristic curves of the half-cell at a scan rate of 50 mV. This suggests that Co helps to reduce the reduction potential for hydrogen either by improving electrocatalytic behavior of Ni or by decreasing the resistance of the Ni-coated electrode. The current–voltage characteristic curves of the half-cell at a scan rate of 50 mV s^{-1} of the respective electrodes are shown in Fig. 7. The maximum current density (300 mA cm^{-2}) is found for the Ni–Co (90:10) electrode. For electrode Ni–Fe (90:10), a maximum current density of around 267 mA cm^{-2} was recorded, whereas 250 mA cm^{-2} was observed only in the case of the Ni electrode. This shows a 20% increment of current density for Ni–Fe (90:10) electrodes as compared with Ni only.

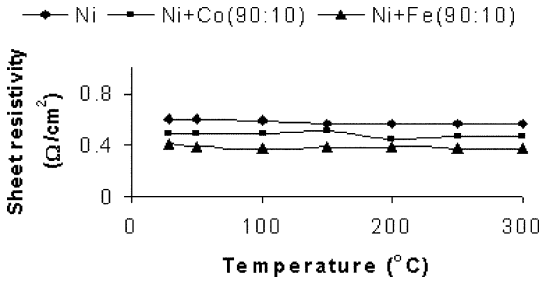

Fig. 6. Variation of sheet resistivity with temperature.

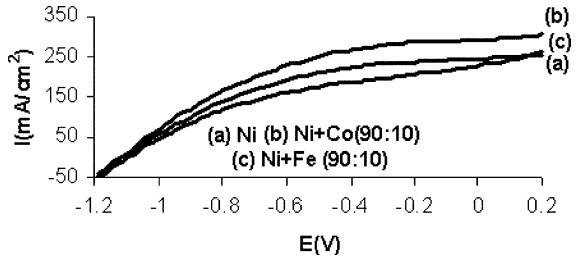

Fig. 7. Half-cell current–voltage characteristics at scan rate 50 mV S^{-1} for carbon beads electrode in 30% KOH solution SCE used as reference electrode.

Table 1
Comparison of different carbon beads electrodes

Electrode	Sheet resistivity ($\Omega\,cm^2$)	H_2 dissociation voltage (mV)	I_{max} ($mA\,cm^{-2}$) for half-cell at scan rate $50\,mV\,s^{-1}$	I_{stable} ($mA\,cm^{-2}$) for half-cell chrono-potentiometry at 0.2 V	I_{max} ($mA\,m^{-2}$) for full-cell at scan rate $50\,mV\,s^{-1}$	I_{stable} ($mA\,cm^{-2}$) full-cell chrono-potentiometry at 0.9 V	Maximum power ($mW\,cm^{-2}$ at 0.9 V)
AB1 (carbon beads + Ni)	0.599	−956	250.38	143.36	223.6	191	171.90
AB2 (carbon beads + Co)	0.420	−713	167.31	52.96	80.29	69.39	162.45
AB3 (carbon beads + Fe)	0.302	−698	132.73	48.72	64.23	42.77	38.49
AB4 (carbon beads + Ni (90% + Co (10%)))	0.490	−982	300.17	169.56	276.64	204.13	183.72
AB5 (carbon beads +Ni (50% + Co (50%)))	0.396	−873	234.21	151.71	202.19	170.14	153.13
AB6 (carbon beads +Ni (10% + Co (90%)))	0.258	−753	190.43	68.14	123.23	100.71	90.64
AB7 (carbon beads +Ni (90% + Fe (10%)))	0.408	−961	267.74	149.21	265.61	193.63	174.23
AB8 (carbon beads + Ni (50% + Fe (50%)))	0.116	−853	207.28	137.03	136.42	103.17	92.85
AB9 (carbon beads + Ni (10% + Fe (90%)))	0.116	−703	167.28	57.03	86.42	73.17	65.85

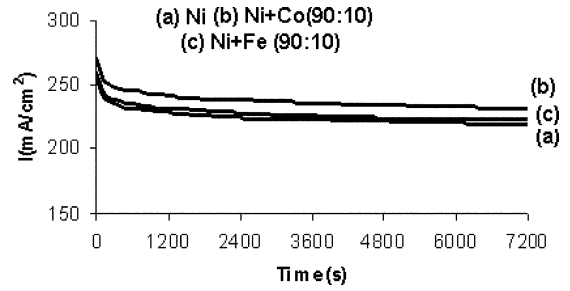

Fig. 8. Half-cell chrono-potentiometric characteristics curves at 0.2 V for carbon beads electrode.

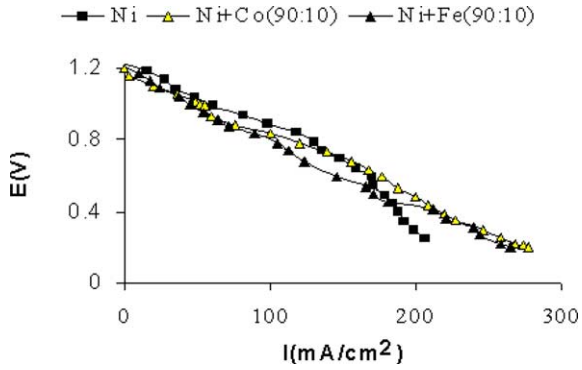

Fig. 9. Full-cell current–voltage curves at scan rage of $5\,mV\,s^{-1}$ for AFC using carbon beads electrode with different metal and Ag oxygen electrode.

The half-cell chrono-potentiometry was recorded at 200 mV and its characteristic curve is shown in Fig. 8. The stable current density observed for Ni–Co (90:10) electrode is $170\,mA\,cm^{-2}$ compared with of 53 and $49\,mA\,cm^{-2}$ for Fe and Co electrodes, respectively. For only Ni, value is $143\,mA\,cm^{-2}$. Full-cell characteristics of the electrodes are presented in Fig. 9. Here a maximum current density of 277, 266, $224\,mA\,cm^{-2}$ is recorded for Ni–Co (90:10) Ni–Fe (90:10) and Ni, respectively. Among the different proportions of bimetallic electrode, Ni–Ce (90:10) and Ni–Fe (90:10) show the best performance. It is therefore suggested that addition of small amounts of Co and Fe to Ni help to increase the conduction. The may also reduce the particle size of the active electrocatalytic sites. As a

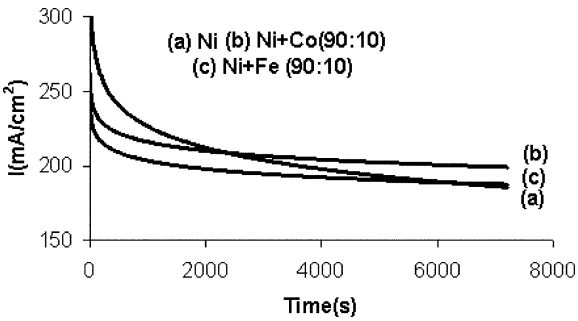

Fig. 10. Full-cell chrono-potentiometric curves at 0.9 V for AFC using carbon beads electrode with different metal and Ag oxygen electrode.

result, the surface area available for chemisorption of H_2 increases, which further improves the catalytic activity. This reasoning is also supported by the chrono-potentiometry curve shown in Fig. 10. From the characteristic curve, it can be inferred that addition of minor amounts of Co or Fe, with Ni as electrocatalyst enhances the catalytic activity. Moreover, it is also clear that addition of a large amount of Co hinders the catalytic activity of Ni.

4. Conclusions

A bimetallic electrocatalyst deposited over carbon beads gives an improved performance compared to that of a mono metal catalyst. Addition of Co and Fe with Ni enhances the electrochemical characteristics. This is probably due to the alloy formation and surface reconstruction effects of the binary electrocatalysts. Among the different compositions Ni–Co (90:10) is found to be most effective and an almost 7% increment in power density is recorded for this electrode compared with a Ni electrode.

Acknowledgements

A.K. Chatterjee acknowledges the financial support provided by Ministry of Non-conventional Energy Sources, Government. of India, to conduct the research work. At the authors acknowledge the help rendered by RSIC and the Department of Earth Science of IIT-Bombay for analysis of the samples.

References

[1] S.A. Boudghene, E. Traversa, Renewable Sustainable Energy Rev. 6 (2002) 295–304.
[2] A.J. Appleby, Energy 2 (1996) 521–653.
[3] G. F McLean, T. Niet, S. Prince-Richard, N. Djilali, Int. J. Hydrogen Energy 27 (2002) 507–526.
[4] K. Kordesch, V. Hacker, J. Gsellmann, M. Cifrain, G. Faleschini, P. Enzinger, R. Fankhauser, M. Ortner, M. Muhr, R.R. Aronson, J. Power Sources 86 (2000) 162–165.
[5] Joongpyo Shim, H.-K. Lee, Mater. Chem. Phys. 69 (2001) 72–76.
[6] M. Schulze, E. Gulzow, G. Steinhilber, Appl. Surf. Sci. 179 (2001) 251.
[7] E. Han, I. Ero, G. lu, L. Turker, Int. J. Hydrogen Energy 25 (2000) 157.
[8] E. Gulzow, M. Schulze, G. Steinhilber, J. Power Sources 106 (2002) 126.
[9] M. Schulze, E. Gulzow, G. Steinhilber, Appl. Surf. Sci. 179 (2001) 251.
[10] A.K. Chatterjee, M. Sharon, R. Banerjee, J. Power Sources 117 (2003) 39–44.
[11] N.M. Morkovie, P.N. Ross, J. Surf. Sci. Rep. 45 (2002) 117–229.
[12] B.C. Gates, H. Knozinger, Advances in Catalysis, Academic Press, New York, 1998, p. 46.